Data Repository for the magmatic plumbing system of a large Permian caldera exposed to a depth of 25 kilometers

J.E. Quick[1], S. Sinigoi[2], G. Peressini[2], G. Demarchi[2], J. Wooden[3] & A. Sbisà[2]

[1]*Present Address, Southern Methodist University, Dallas, Texas*

[2]*DST-Universita di Trieste, via Weiss 8, 34127 Trieste, Italia*

[3]*United States Geological Survey, Menlo Park, California*

CONTENTS

SHRIMP Geochronology

U-Pb ages were measured on zircon separates from the Sesia-Valley volcanic rocks and Ivrea-Verbano-Zone granitic rocks in three sessions in 2001, 2006 and 2008 at the U.S. Geological Survey/Stanford SHRIMP II RG laboratory at Stanford University. Mineral separation, analytical, and data reduction procedures were identical to those described previously by Peressini et al. (2007) to obtain U-Pb zircon ages for the Mafic Complex. Results are reported in Tables A1 and A2, and on $^{207}Pb/^{206}Pb$-$^{238}U/^{206}Pb$ diagrams in Figures A1 to A8, and summarized in Table A3. The analytical sessions during which the data were acquired are specified in Tables A1 and A2.

Volcanic Rocks

Rhyolite R4: The sample is a dense rhyolitic porphyry with inclusions of glomerophyric feldspars $\leq$ 2 mm collected approximately 1.5 km east of the upper Valle Mosso Granite.

48 spots were analyzed in two sessions (23 in 2006, 25 in 2008). Of these, 33 (17 in 2006, 16 in 2008) were analyzed on stubby prisms (zircon fraction R4S) and 15 (7 in 2006, 8 in 2008) on elongated crystals (zircon fraction R4E). 18 spots analyses yielded a ^{204}Pb-signal below detection limit *(spots R4S-2, R4S-5, R4S-7, R4S-9, R4S-10, R4S-11, R4S-16, R4E-3, in the 2006 run; R4ER-1, R4ER-6, R4R-2, R4R-5, R4R-7, R4R-10, R4R-11, R4R-14, R4ERst-5, R4ERst-8)*, consistent with a low-Pb_{com} content of the zircon population.

The U content of all the analyzed spots varies between 112 and 588 ppm.
Two zircon populations were mounted separately based on morphologic features. The two groups result well distinguished in a Th/U versus U plot (Fig. A1d). Age calculation performed on each group yields distinct age results, which, although within analytical error of one another, are considered separately in the following based on the fact that morphological and geochemical features identify the two groups as effectively distinct zircon populations.

One inherited core age was detected (R4s-13, 573.9±6.0, 1σ) and discarded from age calculation. The high Pb_{com} contents of spots R4R-8 (7.47%) and R4R-12 (1.53% PbCom) led to the exclusion of the two analyses from further consideration. A single-spot analyses yielded a Triassic age record (R4R-9, 236.0±5.4, 1σ), and another single spot analyses yielded a poorly defined Carboniferous age record (R4R-3, 317.2±15.1, 1σ). Both age records may be relevant in the geological history of the Ivrea-Verbano-Massiccio dei Laghi, but do not pertain to the main (Permian) data-set discussed in this paper. Therefore, these two spot-ages are discarded from age calculation, but the presence of older, Carboniferous ages in the zircons from the volcanic rocks is taken into account in interpreting age distributions such as those of spots R4ERst-8, yielding a discordant age of 304.2±7.4 Ma (1σ), and R4ERst-5, yielding an age of 290.3±6.7 Ma (1σ), which represent outliers of the stubby-zircons group. Similarly, the presence of younger, Triassic ages in the zircons from the sample is taken into account in interpreting age distributions such as those of spots R4R-4, yielding an age of 264.2±6.3 Ma (1σ), and R4S-12, yielding a reverse discordant age of 259.0±3.3 Ma (1σ), which represent outliers easily attributed to Pb-loss and discarded from age calculation.

Elongated zircons: 15 age data collected on elongated zircons are (sub-) concordant and yield a weighted average age of 285.5 ±4.3 Ma (95% c.l., n=15, MSWD = 2.9, Probability = 0.000). Spots R4E-1 and R4E-4 , which yielded ages of 275.5 ±3.4 and 275.3 ±3.0 Ma, respectively, are regarded as younger outliers when compared to the elongated zircons group.

Discarding these two spots from age calculation, the resulting $^{206}Pb/^{238}U$ weighted average age is **289.1±2.7** Ma (2s, n=13, MSWD = 1.20, Probability = 0.28), which we consider the best estimate for the age of this zircon group.

Stubby zircons: 30 age data collected on stubby zircons are (sub-)concordant. Rejection of spot 4s11b (younger outlier) returns a weighted average age of **281.7 ±2.6** Ma (95% c.l., n=29, MSWD = 2.4, Probability = 0.000) , which we consider the best estimate for the age of this zircon group.

Figure A1. Age plots for sample R4: (A) cumulative probability; (B) ^{206}Pb-^{238}U weighted average with rejected data shown as open, numbered rectangles; (C) $^{207}Pb/^{206}Pb$-$^{238}U/^{206}Pb$ Tera-Wasserburg plot of the two zircon groups at the 1s level; (D) Th/U vs U plot.

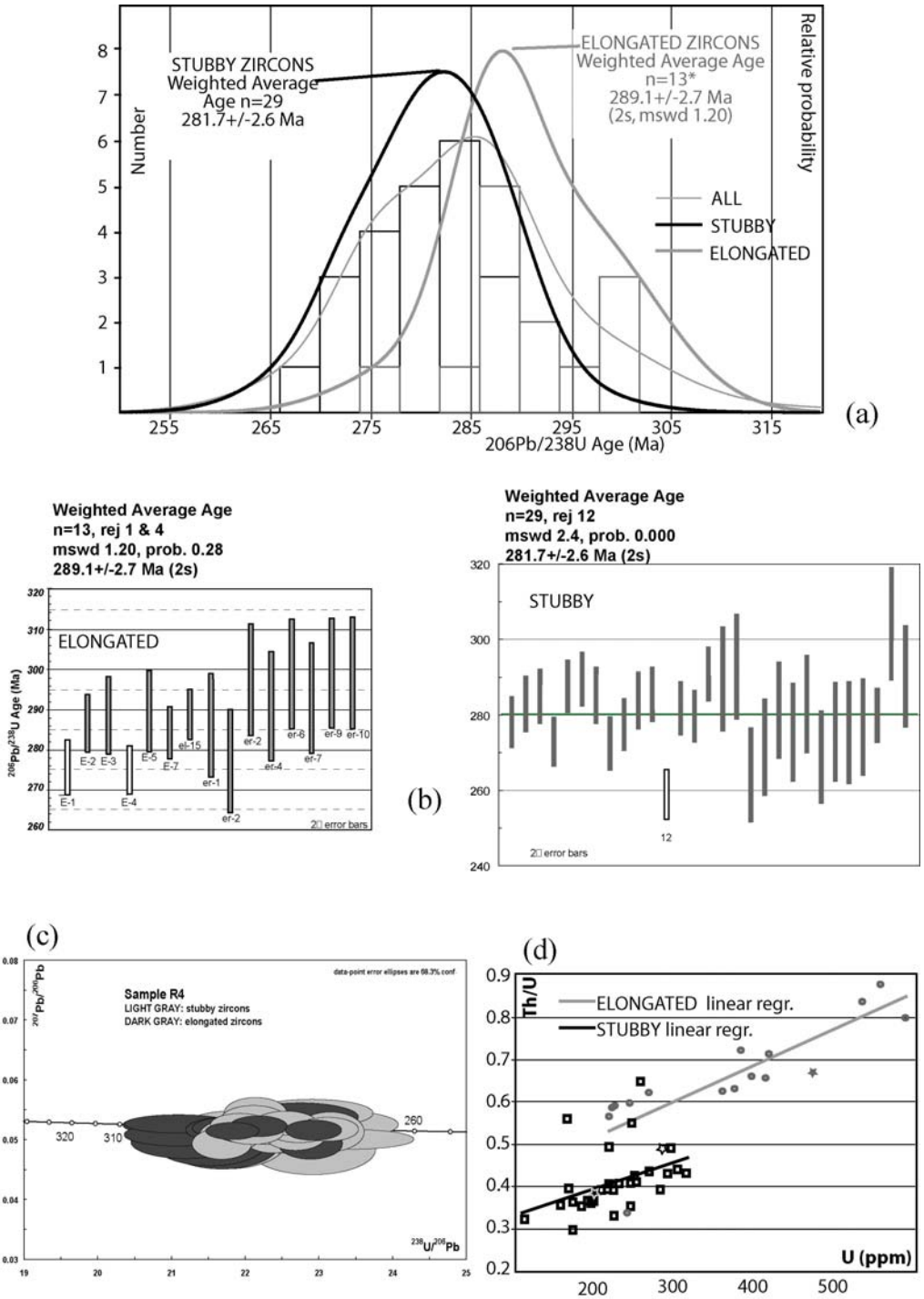

<u>Andesitic Basalt R6</u>: The sample is an inclusion-free, andesitic-basalt flow intercalated with rhyolite approximately 1.5 km east of the upper Valle Mosso Granite. The sample is inferred to

have been taken near the deeper exposed levels of the volcanic section based on attitudes in the section and on overlying Mesozoic sedimentary rocks.

27 spots were analyzed in a single session in 2006. Among these, spots R6-9 and R6-23 were identified by the reduction software as having negative percentage of $^{206}Pb_{com}$, a value changed to 0 before age calculations. Nine spot analyses (R6-1, R6-2, R6-4, R6-5, R6-7, R6-11, R6-16, R6-17, R6-21) yielded ^{204}Pb signals below detection limit. Excluding six inherited cores with ages >430 Ma (R6-5, R6-6, R6-18, R6-23, R6-25, R6-27), the U content of the analyzed spots ranged from 48 to 610 ppm, with an average value of 376 ppm, with the exception of one anomalously high value of 1,176 ppm measured for spot R6-26, and Th/U ranged from 0.35 and 0.87, with an average value of 0.53, with the exception of one anomalously high ratio of 1.39 recorded for spot R6-26. Two single spot analyses were rejected because of large errors on isotopic ratios (16%, R6-10; 9%, R6-20) resulting from the lowest 206/204 ratios measured for this sample (490 and 2877, respectively).

The intercept age calculated on the 19 remaining spot analyses is 287.8 ±2.7 Ma (95% confidence, n=19, MSWD = 1.8), coincident with the $^{206}Pb/^{238}U$ weighted average age 287.3±2.6 Ma (95% conf., n=19, MSWD = 2.6, Probability = 0.000).

A single spot analysis yielded an age of 297.1±3.7 (1σ, R6-2), which represents an outlier. Similarly, ages on spots R6-9 and R6-12 (respectively, 278.8 ±3.1 and 275.4 ±3.1, 1σ) are discarded from age calculation as younger outliers. The remaining 16 age data are (sub-)concordant and yield a concordia age of 288.1 ±1.7 Ma (2s, n=16, MSWD = 4.8, Probability = 0.029), coincident with the $^{206}Pb/^{238}U$ weighted average age 288.3±1.7 Ma (2s, n=16, MSWD = 1.05, Probability = 0.40).

Our favourite age for the sample is the concordia value, coincident with the weighted average age of 288±2 Ma.

Figure A2. Age plots for sample R6: (A) cumulative probability;

(B) ^{206}Pb-^{238}U with rejected data shown as open, numbered rectangles; and (C) $^{207}Pb/^{206}Pb$-$^{238}U/^{206}Pb$, with rejected data shown with light-gray fill and condordia age shown with heavy ellipse.

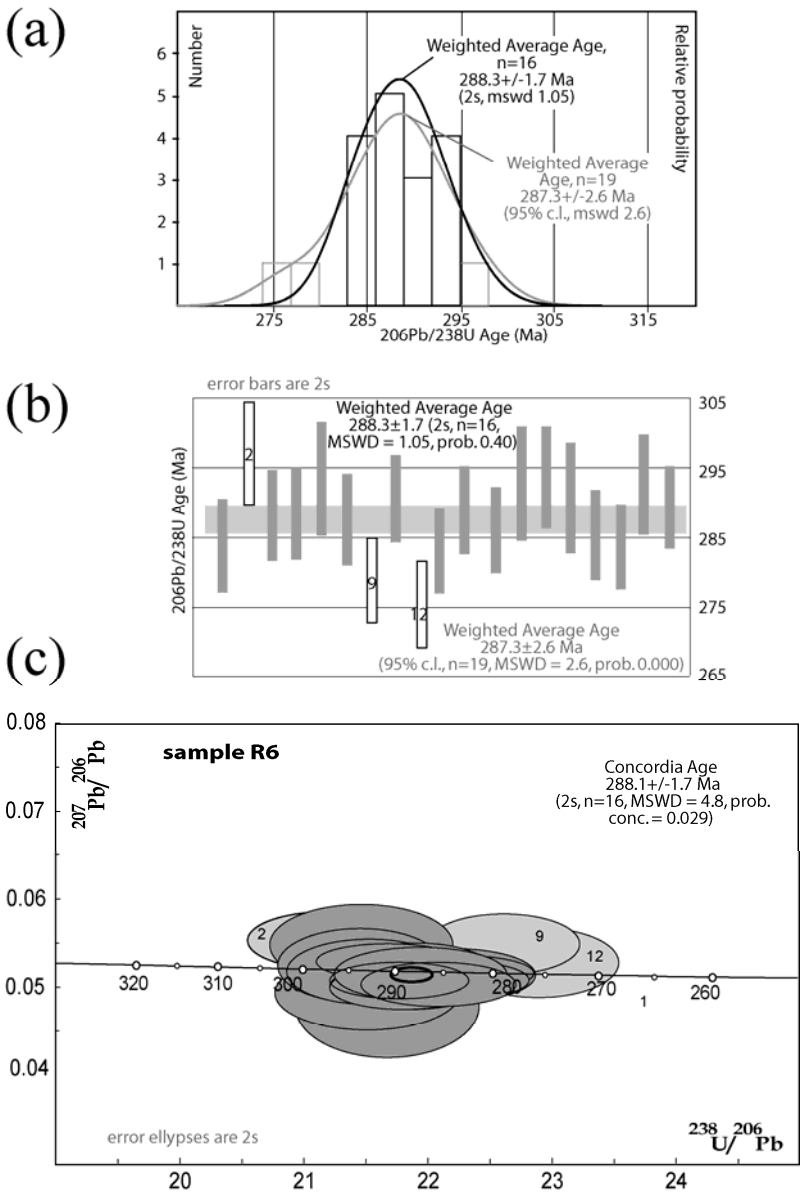

Rhyolite R9: The sample is a dense rhyolite porphyry with inclusions of volcanic rock.

15 spots were analyzed. Spot 13 was attributed by the reduction software to have a negative percentage of $^{206}Pb_{com}$, a value changed to 0 before age calculations. Eight spots analyses yielded a 204-signal below detection limit (spots R9-1, R9-3, R9-4, R9-5, R9-6, R9-9, R9-11, R9-14). No inherited core ages were detected. Although 5 spot analyses yielded U>1,000 ppm (spots R9-1, R9-2, R9-8, R9-12, R9-14), the average U content of the analyzed spots is 777 ppm. The average Th/U is 0.49, with anomalously high values recorded for spots R9-4 (1.01) and R9-11 (0.94).

The dark appearance in cathodoluminescence of the zircons is consistent with the high U content. These images confirm the absence of inherited cores and reveal that most grains are oscillatory zoned but contain inclusions or cracks. Spots R9-7 and R9-10 are rejected from age calculation because they sampled a crack and a recrystallized, thick white rim, respectively. These features explain the relative young and/or discordant ages of the two analyses. The remaining 13 age data are (sub-)concordant but their span 277.9±2.0 (1σ, R9-10) to 293.5±1.8 (1σ, R9-12) does not allow a Concordia age calculation.

The $^{206}Pb/^{238}U$ weighted average age results in an age of 286.3±2.7 Ma (95% conf., n=15, MSWD = 6.3, probability = 0.000), coincident with the regression to Pb_{com} at 280 Ma after Stacey&Kramers (1975) which returns a value of 286.6±2.7 Ma (n=15, MSWD = 6.0). The Isoplot function, Zircon Age Extractor, gives an age of 284.79+3.79/-2.33 Ma (96.1% confidence) on 9 spot analyses. Nonetheless, in light of the results obtained on sample R4, our favourite interpretation of the age-record contained in the zircons of sample R9 is that shown by the cumulative probability plot, which reveals a distribution around two peaks, at about 284 and 290 Ma. We interpret these ages as dating the crystallization of R9 and the earlier crystallization of included antecrysts, respectively.

Figure A3. Age plots for sample R9: (A) cumulative probability;

(B) ^{206}Pb-^{238}U; and (C) $^{207}Pb/^{206}Pb$-$^{238}U/^{206}Pb$. Data rejected from age calculations show with dashes.

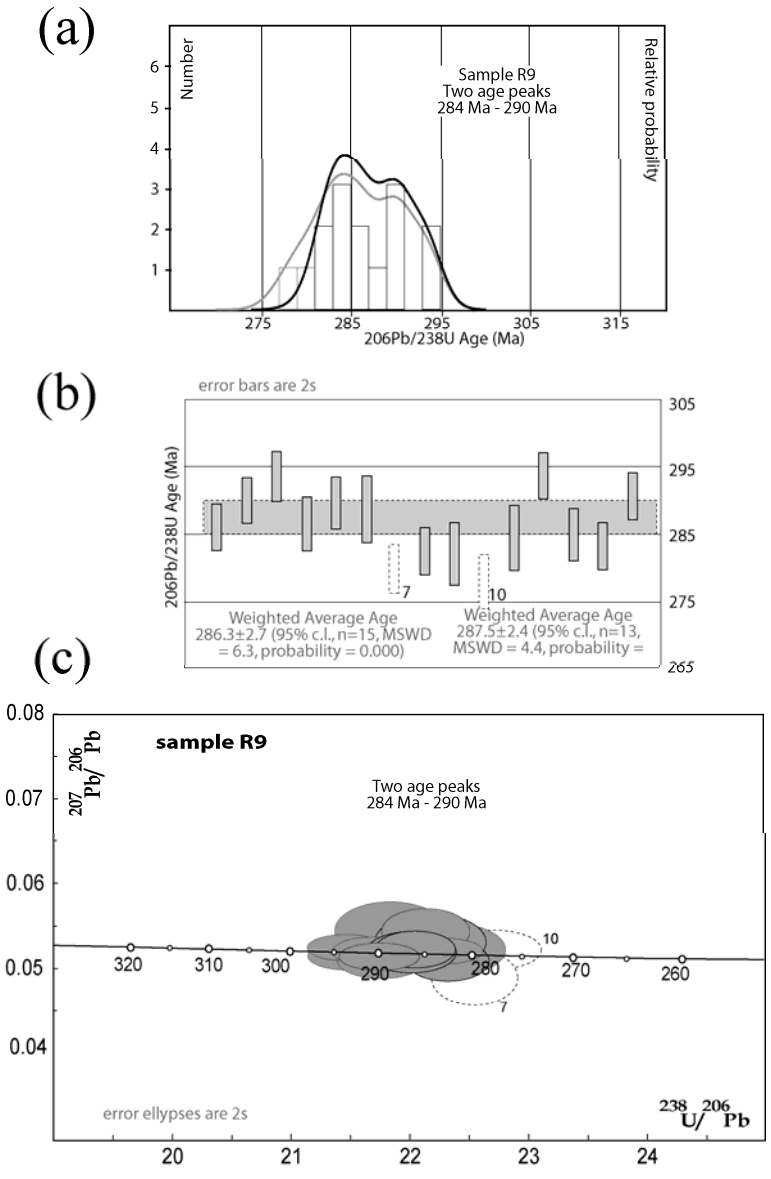

Rhyolite R16: The sample was collected from a block of dense rhyolite porphyry within the caldera megabreccia. The sample is devoid of inclusions.

16 spots were analyzed in a single session. Five spot analyses (R16-4, R16-9, R16-11, R16-12, R16-15), yielded a ^{204}Pb-signal below detection limit. No inherited core ages were detected. The U content of the analyzed spots ranged from 155 and 701 ppm, with an average value of 275 ppm. Th/U of the analyzed spots ranged from 0.33 and 0.90, with an average value of 0.53. All age data are (sub-)concordant and span 273.1±3.6 (1σ, R16-10) to 297.7±3.6 (1σ, R16-15). A concordia age calculated on all analyzed spots is 285.2 ±2.3 Ma (95% confidence, n=16, MSWD = 2.6, Probability = 0.11), which is coincident with a less precise ^{206}Pb/^{238}U weighted average age of 285.0±3.0 (95% conf., n=16, MSWD = 2.6, probability = 0.001). Rejection of spot-analyses R16-1 and R16-10, which have lower precision due to lower U content (the lowest for the sample, 181 and 155 ppm, respectively), and which plot at the youngest end of the distribution, and rejection of the slightly older R16-15 that may be regarded as an outlier, leads to the calculation of a concordia age at 285.3 ±1.9 Ma (2s, n=13, MSWD = 1.4, Probability = 0.24), coincident with the less precise ^{206}Pb/^{238}U weighted average age of 285.3±1.9 (2s, n=13, MSWD = 1.05, probability = 0.39).

The age of the sample is well defined by the concordia age, coincident with the weighted average value of 285±2 Ma.

Figure A4. Age plots for sample R16: (A) cumulative probability; (B) ^{206}Pb-^{238}U with rejected data shown as open, numbered rectangles; and (C) $^{207}Pb/^{206}Pb$-$^{238}U/^{206}Pb$, with rejected data shown with light-gray fill and concordia age shown with heavy ellipse.

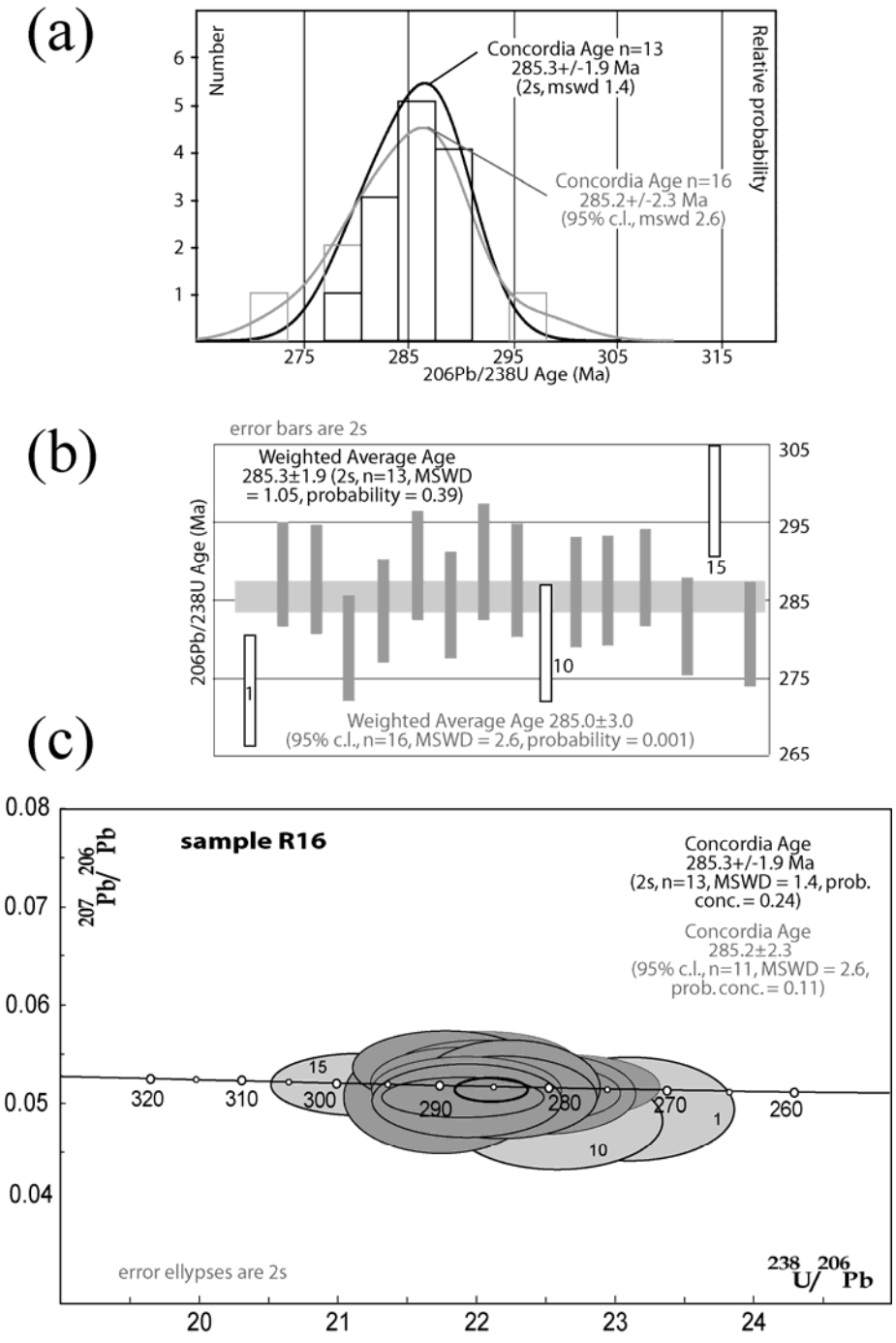

IVR2: 8 spots were analyzed in single session in 2006 and 14 in a single session in 2008. 4 spot analyses (IVR2-1, IVR2r-9, IVR2r-10, IVR2r-13) yielded a ^{204}Pb-signal below detection limit. Inherited cores are clearly visible in cathodoluminescence, but were not analyzed. The U contents ranged from 164 and 392 ppm, with an anomalously high value of 1169 ppm measured for spot IVR2r-4. This spot excluded, the average U content is 260 ppm. Th/U of the analyzed spots varies between 0.34 and 0.58, with an average value of 0.45. Age data display a spread too large to justify the calculation of a single age. Pb_{com} contents in the whole zircon population are high, as shown by the Tera-Wasserburg plot, which is color-coded for Pb_{com} % content.

These problems notwithstanding, the cumulative probability plot shows a distribution around a main peak, which we consider as follows. Four spot analyses (IVR2-8, IVR2r-3, IVR2r-6, IVR2r-7) were rejected because of large errors on isotopic ratios resulting from high-Pb_{com}. The remaining 18 age data are (sub-)concordant and span 277.0±3.6 Ma (1σ, IVR2-4) to 299.6±6.8 Ma (1σ, IVR2r-15), yielding a ^{206}Pb/^{238}U weighted average age of 287.3±3.1 (95% conf., n=19, MSWD = 1.8, probability = 0.016).

However, the age distribution on a cumulative probability plot is very similar to that obtained for sample R9 in that there is evidence in the distribution for two ages, and we consider the most like solution to be an age of approximately 290 Ma dominated by antecrysts and corresponding to the older peak in Figure A5, and a more subtly defined age in the cumulative distribution plot of approximately 284 Ma, corresponding to the crystallization age of the rock .

Figure A5. Age plots for sample IVR2: (A) Weighted average of ^{206}Pb-^{238}U ages with rejected data shown as open, numbered rectangles (B) ^{206}Pb-^{238}U ages cumulative probability; and (C) $^{207}Pb/^{206}Pb$-$^{238}U/^{206}Pb$, color-coded for PbCom% content.

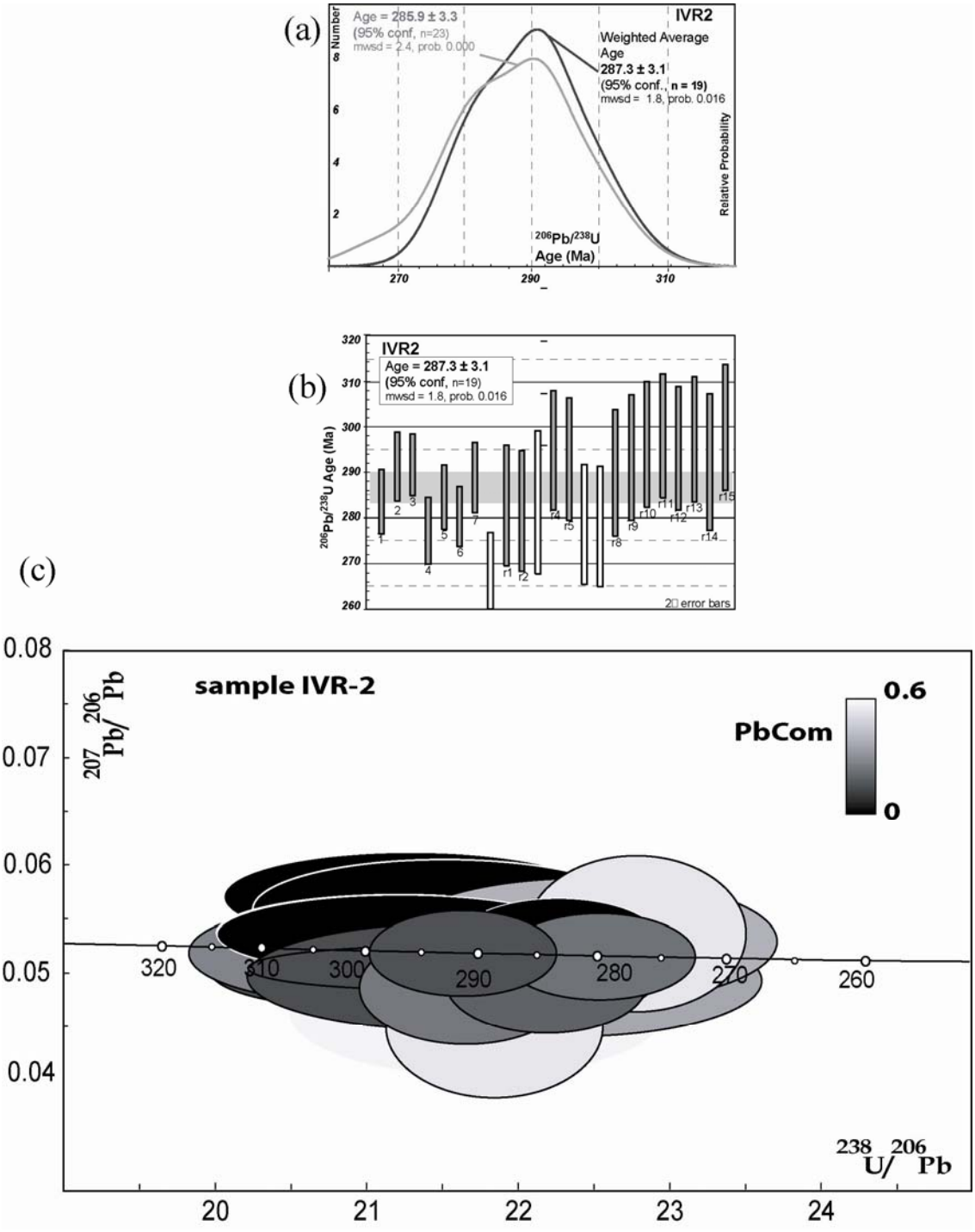

TABLE A1: SHRIMP (II RG) U–Th–Pb isotopic data of zircons from volcanic rocks. bdl=204 below detection limit; 1: inherited core; 2: high U; 3: low Th/U; 4: highly discordant; 5: contains inclusion; 6: outlier; 7: high PbCom and/or large errors; 8 anomalous high Th/U; (*): used to calculate ages reported in figures and text.

Spot	206 204, meas	% comm 206	ppm U	$^{232}Th/^{238}U$	Pb_c-corr 206Pb 238U Age	1s err	% Dis-cor-dant	Total 238 /206	% err	Total 207 /206	% err	$^{238}U/^{206}Pb$	% err	207r /206r	% err	run	notes	age calc
R4E-1	6342	0.29	241	0.34	275.8	3.4	-49	22.81	1.3	.0512	2.6	22.88	1.3	.0489	3.7	06	6	
R4E-2	12569	0.15	225	0.59	286.9	3.6	-10	21.94	1.3	.0525	2.6	21.97	1.3	.0514	3.1	06		*
R4E-3	bdl	0.00	375	0.63	288.8	4.8	-8	21.82	1.7	.0516	2.5	21.82	1.7	.0516	2.5	06		*
R4E-4	9097	0.21	557	0.88	275.3	3.0	-9	22.88	1.1	.0528	1.7	22.92	1.1	.0512	2.2	06	6	
R4E-5	14919	0.13	243	0.60	289.8	5.0	-12	21.72	1.8	.0523	2.5	21.75	1.8	.0513	2.9	06		*
R4E-7	20418	0.09	360	0.63	284.5	3.3	-2	22.15	1.2	.0526	2.1	22.17	1.2	.0519	2.3	06		*
R4e-15	15866	0.12	588	0.80	289.0	3.1	-16	21.78	1.1	.0520	1.7	21.81	1.1	.0510	1.9	06		*
R4ER-1	bdl	0.00	417	0.71	286.3	6.5	-11	22.02	2.3	.0513	2.0	22.02	2.3	.0513	2.0	08		*
R4ER-2	5251	0.36	396	0.66	277.5	6.3	26	22.66	2.3	.0563	2.0	22.74	2.3	.0535	3.0	08		*
R4ER-3	4802	0.39	267	0.62	297.6	6.9	-47	21.08	2.4	.0522	2.5	21.17	2.4	.0492	3.9	08		*
R4ER-4	2688	0.70	222	0.59	290.9	6.9	-52	21.51	2.4	.0543	2.6	21.66	2.4	.0488	5.9	08		*
R4ER-6	bdl	0.00	413	0.66	299.0	6.8	0	21.06	2.3	.0523	2.0	21.06	2.3	.0523	2.0	08		*
R4ER-7	2644	0.71	218	0.56	293.1	7.0	-46	21.34	2.4	.0548	2.8	21.50	2.4	.0492	5.6	08		*
R4ER-9	9020	0.21	534	0.84	299.2	6.7	-29	21.01	2.3	.0520	1.8	21.05	2.3	.0504	2.6	08		*
R4ER-10	48673	0.04	382	0.72	299.1	6.9	-4	21.05	2.4	.0524	2.2	21.05	2.4	.0521	2.3	08		*
R4S-1	6126	0.31	250	0.42	278.2	3.4	-23	22.60	1.2	.0528	2.4	22.67	1.2	.0504	3.5	06		*
R4S-2	bdl	0.00	173	0.30	283.0	3.7	-13	22.28	1.3	.0511	3.0	22.28	1.3	.0511	3.0	06		*
R4S-3	8981	0.21	218	0.40	284.9	3.6	31	22.08	1.3	.0557	2.6	22.13	1.3	.0540	3.5	06		*
R4S-4	16418	0.11	295	0.49	273.0	3.3	-6	23.09	1.2	.0522	2.3	23.11	1.2	.0513	2.6	06		*
R4S-5	bdl	0.00	268	0.43	287.7	3.5	2	21.91	1.2	.0522	2.4	21.91	1.2	.0522	2.4	06		*
R4S-6	5959	0.31	252	0.41	289.5	3.6	-30	21.70	1.3	.0526	2.5	21.77	1.3	.0502	3.6	06		*
R4S-7	bdl	0.00	183	0.35	285.3	3.7	17	22.10	1.3	.0531	2.9	22.10	1.3	.0531	2.9	06		*
R4S-8	4528	0.41	195	0.36	272.5	3.6	-13	23.06	1.3	.0542	2.8	23.16	1.3	.0509	4.4	06		*
R4S-9	bdl	0.00	223	0.39	277.6	3.5	-10	22.73	1.3	.0512	2.7	22.73	1.3	.0512	2.7	06		*
R4S-10	bdl	0.00	168	0.39	283.9	3.8	0	22.21	1.4	.0519	3.1	22.21	1.4	.0519	3.1	06		*
R4S-11	bdl	0.00	218	0.39	285.5	3.6	-18	22.08	1.3	.0509	2.7	22.08	1.3	.0509	2.7	06		*
R4S-12	2475	0.76	246	0.55	259.0	3.3	1	24.21	1.3	.0574	2.5	24.39	1.3	.0514	5.5	06	6	
R4S-13	14710	0.13	473	0.67	573.9	6.0	8	10.73	1.1	.0615	1.1	10.74	1.1	.0605	1.4	06	1	
R4S-14	5474	0.34	224	0.33	281.9	3.5	-28	22.29	1.3	.0529	2.6	22.37	1.3	.0502	3.8	06		*
R4S-16	bdl	0.00	245	0.41	279.8	3.4	8	22.54	1.3	.0524	2.6	22.54	1.3	.0524	2.6	06		*
R4S-17	7188	0.26	257	0.65	290.9	3.6	-52	21.60	1.3	.0509	2.8	21.66	1.3	.0488	3.6	06		*
R4SR-1	2316	0.81	230	0.41	289.6	6.9	-40	21.59	2.4	.0559	2.8	21.77	2.4	.0495	6.6	08		*
R4SR-2	bdl	0.00	244	0.35	292.9	7.0	-18	21.52	2.4	.0510	3.2	21.52	2.4	.0510	3.2	08		*
R4SR-3	2972	0.63	199	0.38	317.2	15.1	4	19.70	4.9	.0579	3.5	19.83	4.9	.0530	5.4	08	1	
R4SR-4	3776	0.50	191	0.36	264.2	6.3	-20	23.78	2.4	.0542	2.8	23.90	2.4	.0503	6.0	08	6	*
R4SR-5	bdl	0.00	165	0.56	271.6	6.4	8	23.24	2.4	.0522	3.0	23.24	2.4	.0522	3.0	08		*
R4SR-6	14206	0.13	315	0.43	281.3	6.4	-20	22.39	2.3	.0517	2.1	22.42	2.3	.0506	2.3	08		*
R4SR-7	bdl	0.00	158	0.35	275.5	6.5	36	22.90	2.4	.0541	2.9	22.90	2.4	.0541	2.9	08		*
R4SR-8	250	7.47	218	0.49	290.3	9.7	126	20.09	2.4	.1193	16.1	21.71	3.4	.0615	45.7	08	7	
R4SR-9	4189	0.45	284	0.49	236.0	5.4	-24	26.70	2.3	.0532	2.3	26.82	2.3	.0497	4.0	08	6	
R4SR-10	bdl	0.00	303	0.44	283.0	6.5	-10	22.29	2.3	.0513	2.2	22.29	2.3	.0513	2.2	08		*
R4SR-11	bdl	0.00	291	0.43	269.0	6.2	-34	23.47	2.3	.0496	2.3	23.47	2.3	.0496	2.3	08		*
R4SR-12	1224	1.53	208	0.39	275.6	6.6	-73	22.54	2.4	.0595	2.5	22.89	2.4	.0475	9.2	08	7	
R4SR-13	2900	0.64	112	0.32	275.5	6.8	-65	22.76	2.5	.0530	3.4	22.91	2.5	.0479	6.1	08		*
R4SR-14	bdl	0.00	224	0.39	276.9	6.4	-12	22.79	2.4	.0510	2.6	22.79	2.4	.0510	2.6	08		*
R4Rs-6	5739	0.33	198	0.36	280.0	3.6	-27	22.45	1.3	.0528	2.8	22.52	1.3	.0502	3.9	06		*
R4Rs-5	bdl	0.00	172	0.36	304.2	7.4	-7	20.70	2.5	.0519	3.1	20.70	2.5	.0519	3.1	06	4	*
R4Rs-8	bdl	0.00	282	0.39	290.3	6.7	55	21.71	2.4	.0559	2.5	21.71	2.4	.0559	2.5	06	6	*

TABLE A1: continued.

R6-1	bdl	0.00	257	0.41	283.8	3.4	-6	22.21	1.2	.0516	2.4	22.21	1.2	.0516	2.4	06		*
R6-2	bdl	0.00	229	0.47	297.1	3.7	44	21.20	1.3	.0554	2.5	21.20	1.3	.0554	2.5	06	6	*
R6-3	21038	0.09	366	0.87	288.2	3.3	-6	21.85	1.2	.0524	2.0	21.87	1.2	.0517	2.2	06		*
R6-4	bdl	0.00	326	0.67	288.6	3.3	-29	21.84	1.2	.0502	2.1	21.84	1.2	.0502	2.1	06		*
R6-5	bdl	0.00	215	0.41	437.1	5.1	-19	14.25	1.2	.0536	2.9	14.25	1.2	.0536	2.9	06	1	
R6-6	19212	0.10	211	0.86	642.3	7.2	-7	9.54	1.2	.0606	1.7	9.54	1.2	.0598	1.8	06	1	
R6-7	bdl	0.00	138	0.40	293.5	4.1	40	21.47	1.4	.0549	3.4	21.47	1.4	.0549	3.4	06		*
R6-8	10192	0.18	401	0.47	287.6	3.3	-1	21.88	1.2	.0534	2.0	21.92	1.2	.0520	2.5	06		*
R6-9	bdl	0.00	475	0.52	278.8	3.1	50	22.68	1.1	.0532	1.7	22.62	1.1	.0551	2.5	06	6	*
R6-10	491	3.81	328	0.37	294.4	3.9	117	20.58	1.2	.0905	8.9	21.40	1.4	.0610	15.9	06	7	
R6-11	bdl	0.00	610	0.57	290.7	3.1	14	21.68	1.1	.0531	1.5	21.68	1.1	.0531	1.5	06		*
R6-12	21875	0.09	398	0.41	275.4	3.1	18	22.89	1.2	.0536	2.9	22.91	1.2	.0529	3.1	06	6	*
R6-13	bdl	0.00	572	0.42	283.1	3.1	-4	22.27	1.1	.0517	1.6	22.27	1.1	.0517	1.6	06		*
R6-14	16322	0.11	510	0.45	289.0	3.1	-31	21.79	1.1	.0510	1.7	21.81	1.1	.0501	2.0	06		*
R6-15	10053	0.19	461	0.35	286.1	3.1	-5	22.00	1.1	.0531	1.7	22.04	1.1	.0517	2.2	06		*
R6-16	bdl	0.00	139	0.68	292.8	4.1	-41	21.52	1.4	.0495	3.5	21.52	1.4	.0495	3.5	06		*
R6-17	bdl	0.00	204	0.42	293.6	3.6	6	21.46	1.3	.0526	3.3	21.46	1.3	.0526	3.3	06		*
R6-18	31410	0.06	187	0.89	745.9	8.3	-4	8.15	1.2	.0636	1.5	8.15	1.2	.0632	1.6	06	1	
R6-19	5527	0.34	136	0.41	290.7	4.0	-66	21.61	1.4	.0507	3.2	21.68	1.4	.0480	5.1	06		*
R6-20	2877	0.65	48	0.49	282.8	5.5	-23	22.15	2.0	.0556	5.4	22.29	2.0	.0505	8.9	06	7	
R6-21	bdl	0.00	380	0.44	285.4	3.2	-24	22.09	1.2	.0505	2.0	22.09	1.2	.0505	2.0	06		*
R6-22	33068	0.06	521	0.37	283.7	3.1	-16	22.21	1.1	.0514	1.6	22.23	1.1	.0509	1.7	06		*
R6-23	bdl	0.00	363	0.06	494.8	5.4	14	12.56	1.1	.0574	1.5	12.53	1.1	.0590	1.9	06	1/3	
R6-24	13701	0.14	226	0.59	292.7	3.6	-2	21.50	1.3	.0531	2.5	21.53	1.3	.0520	2.9	06		*
R6-25	11450	0.16	288	0.10	500.0	5.5	-10	12.38	1.1	.0572	1.5	12.40	1.1	.0559	1.9	06	1/3	
R6-26	10597	0.18	1176	1.39	289.4	3.0	-17	21.74	1.0	.0524	1.1	21.78	1.0	.0510	1.6	06	8	*
R6-27	105040	0.02	934	1.10	644.3	6.3	-7	9.51	1.0	.0600	0.7	9.51	1.0	.0599	0.8	06	1/8	
R9-1	bdl	0.00	1191	0.37	286.0	1.7	6	22.05	0.6	.0524	1.6	22.05	0.6	.0524	1.6	06	2	*
R9-2	23790	0.08	1273	0.39	289.9	1.8	-10	21.72	0.6	.0521	1.1	21.74	0.6	.0514	1.3	06	2	*
R9-3	bdl	0.00	890	0.25	293.4	1.9	-10	21.48	0.7	.0515	1.4	21.48	0.7	.0515	1.4	06		*
R9-4	bdl	0.00	520	1.01	286.4	2.0	0	22.01	0.7	.0520	1.9	22.01	0.7	.0520	1.9	06	8	*
R9-5	bdl	0.00	550	0.44	289.5	2.0	-17	21.77	0.7	.0510	1.7	21.77	0.7	.0510	1.7	06		*
R9-6	bdl	0.00	224	0.70	288.6	2.5	35	21.84	0.9	.0545	2.6	21.84	0.9	.0545	2.6	06		*
R9-7	2758	0.68	895	0.24	279.8	1.8	-46	22.39	0.6	.0544	1.3	22.55	0.7	.0491	2.8	06	4/6	
R9-8	6089	0.31	1123	0.53	282.5	1.7	-15	22.26	0.6	.0534	1.2	22.33	0.6	.0510	1.9	06	2	*
R9-9	bdl	0.00	258	0.41	282.1	2.3	6	22.36	0.8	.0523	2.4	22.36	0.8	.0523	2.4	06		*
R9-10	24553	0.08	517	0.61	277.9	2.0	7	22.68	0.7	.0528	1.7	22.70	0.7	.0523	1.8	06	5/6	
R9-11	bdl	0.00	235	0.94	284.3	2.4	19	22.18	0.9	.0532	2.6	22.18	0.9	.0532	2.6	06		*
R9-12	41186	0.05	1423	0.31	293.5	1.8	6	21.46	0.6	.0529	1.0	21.47	0.6	.0526	1.1	06	2	*
R9-13	bdl	0.00	590	0.44	284.8	1.9	37	22.18	0.7	.0531	1.6	22.14	0.7	.0544	2.0	06		*
R9-14	bdl	0.00	1009	0.40	283.1	1.7	3	22.28	0.6	.0522	1.2	22.28	0.6	.0522	1.2	06	2	*
R9-15	22909	0.08	954	0.31	290.6	1.8	-1	21.67	0.6	.0527	1.2	21.69	0.6	.0521	1.4	06		*

TABLE A1: continued.

R16-1	5046	0.37	181	0.38	273.1	3.6	-38	23.02	1.3	.0524	2.9	23.10	1.3	.0494	4.3	06	4/6	
R16-2	19390	0.10	332	0.73	288.2	3.4	1	21.85	1.2	.0529	2.6	21.87	1.2	.0522	2.8	06		*
R16-3	12897	0.15	226	0.42	287.5	3.6	-27	21.90	1.3	.0515	2.7	21.93	1.3	.0503	3.1	06		*
R16-4	bdl	0.00	254	0.54	278.7	3.4	-1	22.64	1.3	.0518	2.5	22.64	1.3	.0518	2.5	06		*
R16-5	17720	0.11	292	0.56	283.6	3.4	-5	22.21	1.2	.0525	3.6	22.24	1.2	.0517	3.8	06		*
R16-6	13936	0.13	238	0.40	289.4	3.6	23	21.75	1.3	.0547	2.5	21.78	1.3	.0536	2.8	06		*
R16-7	6884	0.27	239	0.51	284.2	3.5	-21	22.12	1.3	.0528	2.5	22.18	1.3	.0507	3.4	06		*
R16-8	3398	0.55	212	0.39	289.8	3.7	-23	21.63	1.3	.0549	2.5	21.74	1.3	.0506	4.7	06		*
R16-9	bdl	0.00	210	0.50	287.4	3.6	-11	21.93	1.3	.0514	2.8	21.93	1.3	.0514	2.8	06		*
R16-10	6213	0.30	155	0.47	279.3	3.8	-60	22.52	1.4	.0506	3.2	22.58	1.4	.0482	4.2	06	4/6	
R16-11	bdl	0.00	214	0.43	285.9	3.6	25	22.05	1.3	.0537	2.7	22.05	1.3	.0537	2.7	06		*
R16-12	bdl	0.00	213	0.33	286.0	3.6	13	22.04	1.3	.0529	2.7	22.04	1.3	.0529	2.7	06		*
R16-13	41918	0.04	701	0.90	287.8	3.1	-22	21.89	1.1	.0510	1.5	21.90	1.1	.0506	1.6	06		*
R16-14	12739	0.15	405	0.70	281.3	3.2	-13	22.38	1.2	.0522	1.9	22.42	1.2	.0511	2.3	06		*
R16-15	bdl	0.00	251	0.80	297.7	3.6	-5	21.16	1.2	.0520	2.4	21.16	1.2	.0520	2.4	06	6	
R16-16	8134	0.23	279	0.43	280.5	3.4	-15	22.43	1.2	.0528	2.3	22.48	1.2	.0510	3.3	06		*
IVR2-1	bdl	0.00	227	0.41	283.3	3.5	14	22.26	1.3	.0528	2.5	22.26	1.3	.0528	2.5	06		*
IVR2-2	7871	0.24	183	0.39	291.0	3.7	-42	21.60	1.3	.0513	2.8	21.66	1.3	.0495	3.5	06		*
IVR2-3	13139	0.14	348	0.52	291.4	3.4	-2	21.60	1.2	.0531	2.0	21.63	1.2	.0520	2.5	06		*
IVR2-4	3474	0.54	197	0.42	277.0	3.6	26	22.65	1.3	.0577	2.6	22.77	1.3	.0535	4.5	06		*
IVR2-5	10346	0.18	239	0.56	284.3	3.5	-35	22.14	1.2	.0512	2.5	22.18	1.2	.0498	3.1	06		*
IVR2-6	8467	0.22	353	0.58	280.0	3.2	-1	22.47	1.2	.0536	2.0	22.52	1.2	.0518	2.6	06		*
IVR2-7	4466	0.42	171	0.38	288.6	3.8	-92	21.75	1.3	.0498	3.0	21.84	1.3	.0465	4.8	06		*
IVR2-8	199	9.41	301	0.56	266.9	5.0	-222	21.43	1.3	.1153	6.9	23.66	1.9	.0404	35.0	06	4/7	
IVR2r-1	5212	0.36	222	0.39	282.5	6.5	-32	22.24	2.4	.0528	2.4	22.32	2.4	.0499	3.6	08		*
IVR2r-2	4774	0.39	210	0.45	281.3	6.5	16	22.33	2.4	.0560	2.4	22.42	2.4	.0530	3.7	08		*
IVR2r-3	167	11.22	286	0.68	283.2	7.8	-142	19.77	2.4	.1327	4.4	22.27	2.8	.0439	30.2	08	4/7	
IVR2r-4	13873	0.13	1169	0.34	294.5	6.5	-19	21.36	2.3	.0520	1.0	21.39	2.3	.0509	1.3	08		*
IVR2r-5	8494	0.22	301	0.48	293.0	6.6	-17	21.46	2.3	.0528	2.0	21.50	2.3	.0510	2.6	08		*
IVR2r-6	972	1.92	252	0.40	278.3	6.5	-15	22.23	2.4	.0660	2.0	22.67	2.4	.0509	7.6	08	7	
IVR2r-7	1045	1.79	200	0.40	277.8	6.6	-20	22.30	2.4	.0647	2.4	22.71	2.4	.0506	8.4	08	7	
IVR2r-8	3260	0.57	222	0.45	289.8	6.9	-60	21.62	2.4	.0528	2.7	21.75	2.4	.0483	4.8	08		*
IVR2r-9	bdl	0.00	164	0.38	292.9	6.9	45	21.52	2.4	.0553	2.8	21.52	2.4	.0553	2.8	08		*
IVR2r-10	bdl	0.00	250	0.43	296.0	6.8	57	21.29	2.4	.0563	2.3	21.29	2.4	.0563	2.3	08		*
IVR2r-11	13618	0.14	392	0.48	297.7	6.7	-23	21.13	2.3	.0518	2.1	21.16	2.3	.0507	2.4	08		*
IVR2r-12	7271	0.26	366	0.50	294.9	6.7	8	21.31	2.3	.0548	2.0	21.37	2.3	.0528	2.6	08		*
IVR2r-13	bdl	0.00	302	0.46	297.0	6.8	18	21.21	2.3	.0535	2.2	21.21	2.3	.0535	2.2	08		*
IVR2r-14	6274	0.30	244	0.44	292.1	7.4	-29	21.51	2.6	.0526	2.4	21.57	2.6	.0503	3.3	08		*
IVR2r-15	6979	0.27	295	0.44	299.6	6.8	-4	20.97	2.3	.0542	2.1	21.02	2.3	.0521	3.0	08		*

Granitic Rocks

Granite CC: The sample was collected from the upper Valle Mosso Granite at Cava Cacciano near the contact with the overlying volcanic rocks.

11 spots were measured during one session in 2008. Spot CC-10 was discarded from the age calculation because of high Pb_{com} content (2.63%) and consequent large errors on calculated ratios (6.8%). Spot CC-5 was discarded because of large errors on calculated ratios resulting from a relatively low U content of 162 ppm coupled with a relatively high Pb_{com} content (0.51%). The remaining 9 spot analyses display in both a cumulative probability plot and a Tera-Wasserburg plot a distribution indicating a typical Pb-loss pattern, with a tail towards younger ages. A concordia age of 273.7 ±2.5 Ma (95% conf., n=9, MSWD = 0.49, prob. Conc. = 0.48) on the 9 spots coincides with the weighted average age of 273.4±2.5 (2σ, n=9, MSWD = 1.7, prob. = 0.091). Additional data rejection performed based on the assumption of Pb-loss leads to the exclusion of spots CC-7 and CC-8, and spot CC-9 because of the strong reverse discordance (-58%). The resulting concordia age of 274.9 ±4.2 Ma (95% conf., n=6, MSWD = 0.95, prob. Conc. = 0.62) is our best estimate for the age of sample CC.

Granite CSB: The sample was collected from the upper Valle Mosso Granite at Cava San Bononio, near the contact with overlying volcanic rocks.

7 spots were measured during a single session in 2008. 3 were discarded from age calculation, as follows. Spots CSB-7 and CSB-5 were discarded from age calculations because of inheritance and high Pb_{com}, respectively. Spot CSB-6, which yielded a U content of 2492 ppm and an age of 296.7±4.1 Ma (1σ), was discarded from age calculations because it represents a clear outlier in the data-set (see cumulative probability plot). The remaining 4 spots define a single age-peak with a gaussian distribution yielding a concordia age of 278.3 ±4.8 Ma (2σ, n=4, MSWD = 0.72, prob. Conc. = 0.29).

A regression based on these same data and on the inherited core age of spot CSB-7 yield a lower intercept of 281.5 +5.3/-5.8 Ma (95%-conf., n=5). Absent additional discordant points to

support the intercept calculation, the Concordia age of 278±5 Ma is our preferred age for this sample.

Figure A6. Age plots for samples CC and CSB: (A) Weighted average of ^{206}Pb-^{238}U ages with rejected data shown as open, numbered rectangles (B) ^{206}Pb-^{238}U ages cumulative probability; and (C) $^{207}Pb/^{206}Pb$-$^{238}U/^{206}Pb$.

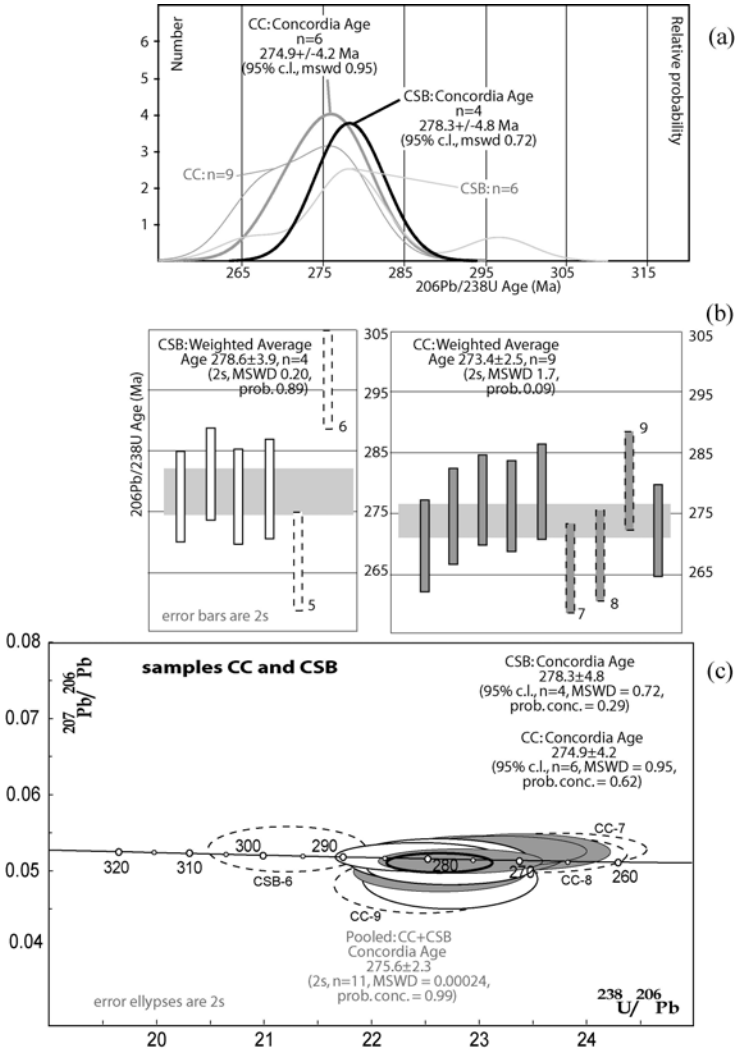

Sample RP: Sample RP was collected in the Roccapietra quarry located in the westernmost Roccapietra Granite.

15 spots were analyzed during a single session in 2008. 2 spot analyses yielded a 204-signal below detection limit (spots RP-4, RP-14). A high Pb_{com} content was attributed to spot RP-3 (1.43%). The average U content of the analyzed spots is 390 ppm. An anomalously high value of

1314 ppm was measured for spot RP-7, and low values were detected for spots RP-3 (74 ppm) and RP-10 (111 ppm). These three spots excluded, the average U content is calculated at 362 ppm, and varies between 141 and 738 ppm.

The average Th/U of the analyzed spots has a value of 0.50. With the exception of spots RP-1 (0.12) and RP-10 (1.00), Th/U varies between 0.30 and 0.91. These two spots excluded, the average value is 0.49. Four spot analyses were considered in detail and eventually discarded from age calculation, as follows: spot RP-1, characterized by a low Th/U (0.12); spot RP-2, characterized by a high percentage of reverse discordance (-75%); spot RP-3, characterized by large errors on isotopic ratios, resulting from both a low U and a high Pb_{com} content (74 ppm and 1.43%, respectively); spot RP-10, characterized by a low U content and a high Th/U (111 ppm and 1.00, respectively).

Figure A7 displays cumulative probability, weighted average and Tera-Wasserburg plots of the 15 spots analyzed for sample RP, with the four spots discussed above highlighted in a lighter shade of grey. Resulting values calculated after data rejection do not differ significantly from those calculated on the whole data-set. Weighted average age using all data is 288.9±2.3 Ma (2σ, n=15, MSWD = 0.73, probability = 0.75), as compared to 289.6±2.6 Ma (2σ, n=11, MSWD = 0.60, probability = 0.82) after data-rejection.

The concordia age calculated on all spots is 289.1 ± 3.3 Ma (95%-conf., Prob. Conc. = 0.875, mswd = 0.86, n=15), which is indistinguishable within error from 289.7 ± 3.5 Ma (95%-conf., Prob. Conc. = 0.741, mswd = 0.72, n=11) obtained after rejection of 4 points with large errors.

We feel confident that the best determination of the age of sample RP is represented by the value of 289 ± 3 Ma resulting from the concordia calculation on all spots.

Figure A7. Age plots for sample RP: (A) Weighted average of ^{206}Pb-^{238}U ages with rejected data shown as open, numbered rectangles (B) ^{206}Pb-^{238}U ages cumulative probability; and (C) $^{207}Pb/^{206}Pb$-$^{238}U/^{206}Pb$.

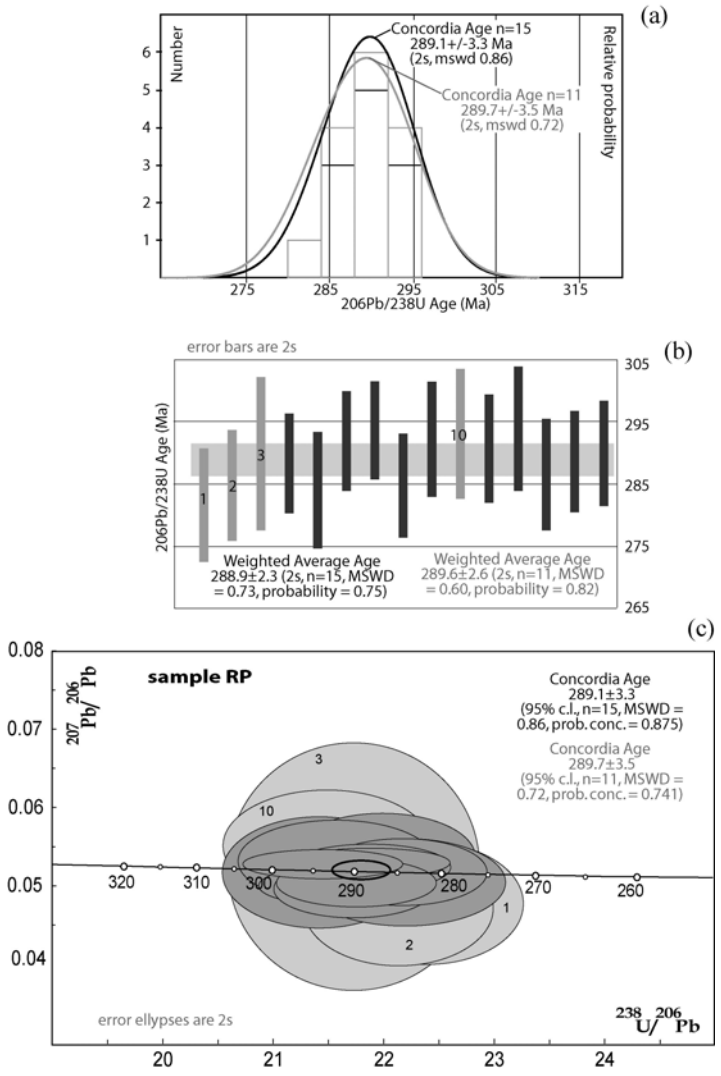

Granite AS: This sample was collected from a small granitic body within the Kinzigite Formation near Alpe Sacchi.

10 spots were analyzed during a single session in 2001. The zircons are extremely dark under cathodoluminescence and no inherited core ages were detected. Most spot analyses are characterized by high values of Pb_{com}, and only four spots analyses yielded $^{206}Pb/^{204}Pb$ >10,000. The U content of the analyzed spots ranged from 4,260 to 13,953 ppm, with an average value of 7,420 ppm, and Th/U of the analyzed spots ranged from 0.003 to 0.065, with an average value of 0.026. Low brightness in cathodoluminescence, high U content, low Th/U, and high Pb_{com} are typical of U-damaged zircon domains, and we interpret the data for this sample to be strongly affected by Pb-loss following metamictization. This is confirmed by two spot analyses, which plot on a discordia line to zero. The remaining data are concordant within error but exhibit a span

of ages too large to justify calculation of a simple concordia age. Excluding one spot on the basis of extremely large errors, we calculate an upper intercept age for this array of analyses of 274+13/-11 Ma with a lower intercept of 16+34/-14 Ma (95% conf., n=9, MSWD =0.53, probability = 0.65).

Figure A8. Concordia plot for sample AS.

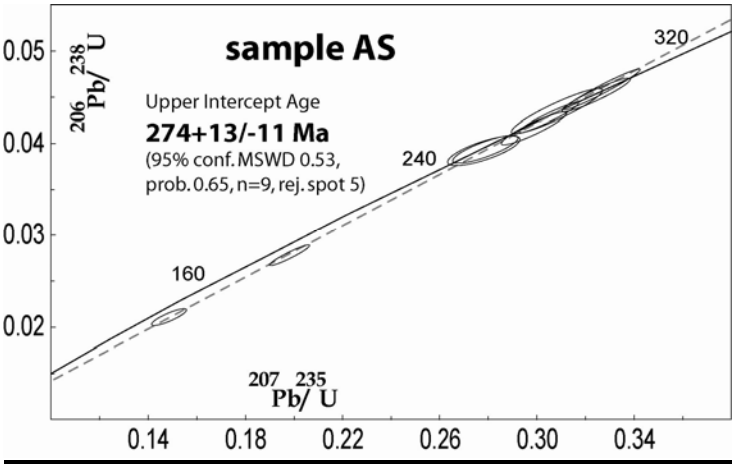

Granite RS: The sample was collected from a small granite body within the Kinzigite Formation on the west back of the Sesia Valley approximately.

21 spots were analyzed in two sessions in 2001 and 2006. Excluding one analysis that sampled a thorite inclusion, the U content ranged from 13 to 2,642 ppm, with an average value of 846 ppm, Th/U of the analyzed spots ranged from 0.02 to 0.85, with an average value of 0.22. Six spot analyses returned inherited ages as old as 2,242±25 Ma, consistent with textures observed under cathodoluminescence indicating the presence of inherited cores. Seven spot analyses yielded either high U (on average 1,558 ppm) and/or low Th/U (on average 0.05), and were skewed to younger ages, suggesting that the zircons suffered Pb loss due to metamictization. Excluding the high-U and low-Th/U analyses, the average U and Th/U are 260 ppm and 0.31, respectively. Disregarding inherited cores analyses, and excluding analyses RS-2 because of its large associated error due to very low U content (13 ppm), and RS-3, characterized by strong discordance, the remaining 13 data are (sub-) concordant and span 248.6±3.6 (1σ, RS-6, core-analyses, most probably result of Pb-loss through recrystallization, suggested by Th/U measured at 0.2) to 290.6±1.7 (1σ, RS-5); this single spot analyses is excluded from calculation, but its age of 291±4 (2s) would be consistent with an origin of the grain as an antecryst.

In the cumulative probability plot, it appears evident that a bimodal age distribution is arranged around a main peak at around 285 Ma, defined by three spot analyses. Together with these 3 concordant spot analyses, the remaining 9 analyses define an upper intercept age of 299±18 (95% conf., n=12, MSWD = 1.3, probability = 0.22) which is mostly conditioned by the oldest concordant three spot analyses (spots RS-1, RS-2, RS-3). The concordia age calculated on these three concordant analyses is 284.3±2.2 Ma (2s, n=3, MSWD = 0.039, Probability 0.84), coincident with the weighted average age of 284.3±2.1 Ma (2s, n=3, MSWD = 0.32, Probability 0.73). The age of 284±2 Ma (2s, n=3) is the best estimate of the age of the granite.

Figure A8. Age plots for sample RS: (A) ^{206}Pb-^{238}U ages cumulative probability; and (B) $^{207}Pb/^{206}Pb$-$^{238}U/^{206}Pb$, dark grey ellipses define the Permian Concordia age, pale grey ellipse represents the antecryst age. White ellipses spread along a Pb loss trend, that defines a Permian upper intercept anchored by three concordant points at 284±2 Ma.

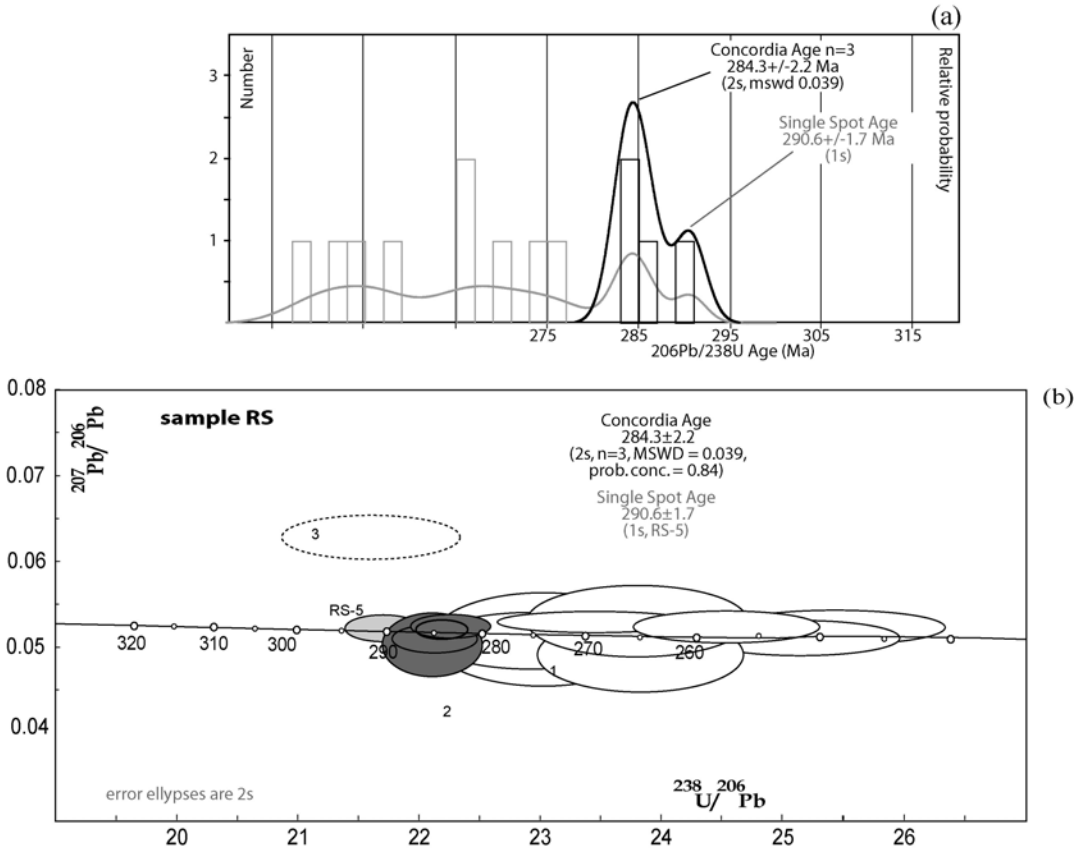

TABLE A2: SHRIMP (II RG) U–Th–Pb isotopic data of zircons from granitic rocks. bdl=204 below detection limit; 1: inherited core; 2: high U; 3: low Th/U; 4: highly discordant; 5: contains inclusion; 6: outlier; 7: high PbCom and/or large errors; 8 anomalous high Th/U; (*): used to calculate ages reported in figures and text.

Spot	206 204, meas	% comm 206	ppm U	$^{232}Th/^{238}U$	Pb_c-corr 206Pb 238U Age	1s err	% Dis-cor-dant	Total 238 /206	% err	Total 207 /206	% err	$^{238}U/^{206}Pb$	% err	207r /206r	% err	run	notes	age calc
CC-1	29964	0.06	424	0.27	269.7	3.8	20	23.39	1.4	.0534	1.6	23.41	1.4	.0529	1.7	08		*
CC-2	24284	0.08	324	0.22	274.5	3.9	9	22.97	1.5	.0529	1.9	22.99	1.5	.0523	2.0	08		*
CC-3	3517	0.53	1803	0.22	277.2	3.7	-5	22.64	1.4	.0557	0.8	22.76	1.4	.0515	2.4	08	2	*
CC-4	35066	0.05	792	0.33	276.2	3.7	-4	22.83	1.4	.0520	1.1	22.84	1.4	.0516	1.2	08		*
CC-5	3663	0.51	162	0.57	266.3	4.0	-30	23.59	1.5	.0538	2.3	23.71	1.5	.0498	4.0	08	7	
CC-6	11596	0.16	317	0.27	278.5	3.9	-27	22.61	1.4	.0514	1.8	22.65	1.4	.0502	2.1	08		*
CC-7	19036	0.10	433	0.57	265.8	3.7	22	23.73	1.4	.0537	1.5	23.75	1.4	.0529	1.7	08		
CC-8	9593	0.19	389	0.30	268.0	3.7	14	23.51	1.4	.0540	1.5	23.56	1.4	.0525	1.9	08		
CC-9	6175	0.30	233	0.35	280.3	4.1	-58	22.43	1.5	.0508	2.0	22.50	1.5	.0484	3.1	08		
CC-10	710	2.63	1965	0.23	276.9	3.8	29	22.19	1.4	.0742	3.6	22.79	1.4	.0536	6.8	08	2/7	
CC-11	bdl	0.00	386	0.60	272.1	3.8	19	23.19	1.4	.0529	1.6	23.19	1.4	.0529	1.6	08		*
CSB-1	8385	0.22	669	0.43	277.4	3.8	-20	22.69	1.4	.0523	1.2	22.74	1.4	.0506	1.8	08		*
CSB-2	bdl	0.00	523	0.33	281.1	3.8	2	22.44	1.4	.0520	1.3	22.44	1.4	.0520	1.3	08		*
CSB-3	4030	0.46	275	0.47	277.4	4.0	-44	22.64	1.5	.0528	1.8	22.74	1.5	.0492	3.3	08		*
CSB-4	13744	0.14	250	0.27	278.6	4.1	-3	22.61	1.5	.0527	2.0	22.64	1.5	.0517	2.3	08		*
CSB-5	299	6.26	434	0.37	266.7	4.1	-94	22.19	1.4	.0958	2.8	23.67	1.6	.0464	13.0	08	7	
CSB-6	2416	0.77	2492	0.26	296.7	4.1	11	21.06	1.4	.0591	1.8	21.23	1.4	.0530	2.3	08	2/6	
CSB-7	26094	0.07	227	0.42	1206.5	21.0	61	4.86	1.9	.1195	0.9	4.86	1.9	.1190	0.9	08	1	
RP-1	2208	0.85	223	0.12	281.8	4.5	-68	22.19	1.6	.0545	2.8	22.38	1.6	.0478	6.6	08	3	*
RP-2	2026	0.92	294	0.30	284.8	4.4	-75	21.93	1.6	.0547	2.5	22.14	1.6	.0475	6.5	08	4	*
RP-3	1310	1.43	74	0.41	289.9	6.1	6	21.43	2.1	.0637	6.1	21.74	2.2	.0525	12.3	08	7	*
RP-4	bdl	0.00	738	0.38	288.4	4.0	14	21.86	1.4	.0530	1.4	21.86	1.4	.0530	1.4	08		*
RP-5	4446	0.42	141	0.38	284.1	4.7	-21	22.10	1.7	.0539	3.1	22.20	1.7	.0506	4.4	08		*
RP-6	6940	0.27	731	0.38	291.9	4.0	-29	21.53	1.4	.0524	1.4	21.58	1.4	.0502	2.1	08		*
RP-7	23808	0.08	1314	0.48	293.8	3.9	11	21.43	1.4	.0536	1.3	21.45	1.4	.0529	1.5	08	2	*
RP-8	8045	0.23	390	0.43	284.8	4.1	-2	22.09	1.5	.0537	2.9	22.14	1.5	.0519	3.4	08		*
RP-9	5978	0.31	205	0.81	292.2	4.6	22	21.50	1.6	.0561	2.8	21.56	1.6	.0537	3.6	08		*
RP-10	3521	0.53	111	1.00	293.1	5.2	43	21.38	1.8	.0593	3.5	21.50	1.8	.0552	5.3	08	5/8	*
RP-11	10341	0.18	304	0.43	290.7	4.3	-24	21.64	1.5	.0520	2.3	21.68	1.5	.0506	2.7	08		*
RP-12	3426	0.55	146	0.91	293.9	5.0	-5	21.32	1.7	.0561	3.2	21.44	1.7	.0518	5.6	08		*
RP-13	3377	0.55	239	0.44	286.6	4.5	20	21.87	1.6	.0577	2.6	22.00	1.6	.0534	4.6	08		*
RP-14	bdl	0.00	496	0.52	288.6	4.1	5	21.84	1.4	.0524	2.4	21.84	1.4	.0524	2.4	08		*
RP-15	4239	0.44	438	0.47	290.0	4.2	-18	21.64	1.5	.0544	2.0	21.74	1.5	.0509	4.0	08		*

TABLE A2: continued.

Spot	206/204, meas	% comm 206	ppm U	$^{232}Th/^{238}U$	Pb_c-corr $^{206}Pb/^{238}U$ Age	1s err	% Dis-cor-dant	Total 238/206	% err	Total 207/206	% err	$^{238}U/^{206}Pb$	% err	207r/206r	% err	run	notes	age calc
AS-1	55871	0.03	4221	0.07	263.0	4.5	10	24.01	1.7	.0523	0.6	24.02	1.7	.0521	0.7	01	2/3	*
AS-2	2841	0.66	13953	0.01	134.4	2.3	83	47.14	1.7	.0563	0.4	47.45	1.7	.0511	1.0	01	2/3/6	
AS-3	15674	0.12	13611	0.01	176.8	2.8	54	35.93	1.6	.0526	0.4	35.97	1.6	.0517	0.5	01	2/3	*
AS-4	60931	0.03	5952	0.02	270.1	4.3	0	23.36	1.6	.0519	0.5	23.37	1.6	.0517	0.5	01	2/3	*
AS-5	554	3.38	5232	0.02	281.1	4.6	-5	21.68	1.6	.0781	2.6	22.44	1.7	.0516	7.9	01	2/3	*
AS-6	3450	0.54	10211	0.003	274.6	6.2	-7	22.85	2.3	.0556	0.4	22.98	2.3	.0513	0.9	01	2/3	*
AS-7	25422	0.07	1364	0.06	248.9	4.0	4	25.39	1.6	.0520	1.1	25.41	1.6	.0514	1.2	01	2/3	*
AS-8	85751	0.02	9213	0.003	291.5	4.6	-8	21.62	1.6	.0518	0.4	21.62	1.6	.0516	0.4	01	2/3	*
AS-9	34308	0.05	4260	0.01	285.4	4.6	0	22.08	1.6	.0524	0.5	22.09	1.6	.0520	0.6	01	2/3	*
AS-10	3947	0.47	6182	0.06	248.0	3.9	5	25.38	1.6	.0551	0.8	25.50	1.6	.0514	1.4	01	2/3	*
RS-1	5634	0.33	130	0.85	604.5	8.4	14	10.14	1.4	.0651	1.6	10.17	1.5	.0625	2.8	01	1	
RS-2	bdl	0.00	13	0.38	269.6	7.2	161	23.41	2.7	.0629	8.6	23.41	2.7	.0629	8.6	01	7	
RS-3	bdl	0.00	283	0.11	291.7	3.9	142	21.61	1.4	.0629	1.7	21.61	1.4	.0629	1.7	01	3/4	
RS-4	173782	0.01	336	0.14	2242.1	24.8	12	2.40	1.3	.1650	0.6	2.40	1.3	.1649	0.6	01	1/3	
RS-5	20615	0.09	1343	0.06	1599.8	26.0	19	3.55	1.8	.1176	1.2	3.55	1.8	.1169	1.3	01	1/2/3	
RS-6	bdl	0.00	535	0.02	248.6	3.6	22	25.43	1.5	.0524	1.5	25.43	1.5	.0524	1.5	01	3	*
RS-7	6103	0.31	207	0.30	265.1	3.8	-40	23.75	1.4	.0517	2.4	23.82	1.5	.0493	3.6	01		*
RS-8	bdl	0.00	149	0.19	275.3	4.0	-14	22.92	1.5	.0509	2.6	22.92	1.5	.0509	2.6	01	3	*
RS-9	bdl	0.00	89	0.57	274.1	4.4	-12	23.02	1.6	.0510	4.4	23.02	1.6	.0510	4.4	01		*
RS-10	42128	0.04	2499	0.18	255.0	3.2	23	24.77	1.3	.0530	0.7	24.79	1.3	.0527	0.7	01	2/3	*
RS-11	11334	0.17	998	0.02	251.5	3.3	0	25.10	1.3	.0525	1.2	25.14	1.3	.0512	1.7	01	3	*
RS-12	21324	0.09	680	0.11	594.3	8.3	10	10.35	1.5	.0620	1.3	10.36	1.5	.0613	1.4	01	1/3	
RS-13	bdl	0.00	135	0.68	265.4	4.1	26	23.80	1.6	.0531	3.2	23.80	1.6	.0531	3.2	01		*
RS-14	6026	0.31	25	3.34	1794.0	27.7	1	3.11	1.8	.1134	1.7	3.12	1.8	.1111	2.0	01	1/5/8	
RS-15	bdl	0.00	1197	0.02	269.2	3.7	23	23.45	1.4	.0531	1.0	23.45	1.4	.0531	1.0	01	2/3	*
RS-16	4597	0.41	2642	0.02	257.6	3.3	18	24.43	1.3	.0556	0.7	24.53	1.3	.0524	1.3	01	2/3	*
RS-1r	16993	0.11	372	0.18	285.2	2.1	-25	22.08	0.8	.0513	2.7	22.11	0.8	.0504	3.0	06	3	*
RS-2r	bdl	0.00	1554	0.07	283.3	1.7	10	22.26	0.6	.0526	1.1	22.26	0.6	.0526	1.1	06	2/3	*
RS-3r	51908	0.04	834	0.11	284.9	1.8	-14	22.12	0.7	.0514	1.3	22.13	0.7	.0511	1.4	06	3	*
RS-4r	35331	0.05	237	0.42	647.1	4.7	2	9.47	0.8	.0621	1.7	9.47	0.8	.0616	1.7	06	1	
RS-5r	18505	0.10	1481	0.02	290.6	1.7	2	21.67	0.6	.0530	1.0	21.69	0.6	.0522	1.2	06	2/3	*

TABLE A3: Summary of SHRIMP (II RG) U–Th–Pb ages for granitic and volcanic rocks.

Sample	Age (Ma)	2s error	Age type	# (rej.)	MSWD	Interpretation	Sample's field name
VOLCANICS							
single age peak							
R6	**288**	**2**	Weighted Average	16 (11)	1.05	*magmatic zircons' age*	
	288	**2**	Concordia	16 (11)	4.8	*magmatic zircons' age*	
R16	**285**	**2**	Concordia	13 (3)	1.4	*magmatic zircons' age*	
multiple age peaks							
R4-elongated	**289**	**3**	Weighted Average	13 (2)	1.2	*antecrysts' age*	
R4-stubby	**282**	**3**	Weighted Average	29 (1)	2.4	*magmatic zircons' age*	
R9	288	2	Weighted Average	13 (2)	4.4	*antecrysts' minimum age*	
	290	-	estimated	6	-	*antecrysts' age*	
	284	-	estimated	7	-	*magmatic zircons' age*	
IVR2	287	3	Weighted Average	19 (4)	1.8	*antecrysts' minimum age*	
	290	-	estimated	-	-	*antecrysts' age*	
	284	-	estimated	-	-	*magmatic zircons' age*	
GRANITES							
single age peak							
CSB	**278**	**5**	Concordia	4 (3)	0.72	*magmatic zircons' age*	Cava San Bononio
CC	**275**	**4**	Concordia	6 (5)	0.95	*magmatic zircons' minimum age*	Cava Cacciano
RP	**289**	**3**	Concordia	15 (0)	0.86	*magmatic zircons' age*	PST-ROC-A-187
AS	**274**	**+13/-11**	Upper Intercept	9 (1)	0.53	*magmatic zircons' minimum age*	Alpe Sacchi
multiple age peaks							
RS	**291**	**2**	Single Spot age	1 (20)	-	*antecrysts' age*	Ronchi Sesia
	284	**2**	Concordia	3 (18)	0.04	*magmatic zircons' age*	

Reconstruction of the pre-Alpine crustal section

Figure A3 presents steps in the removal of Alpine and Mesozic deformation in the southern Ivrea-Verbano Zone and Serie dei Laghi to reconstruct the Early Permian crustal section shortly after caldera formation. Steps are as follows.

(A) Present-day conditions, which correspond to those of the geologic map in Figure 1. Most attitudes on foliation and layering in Ivrea-Verbano Zone dip steeply (Quick et al., 2003). Based on this observation, results from geobarometry (Demarchi et al., 1998) and the structure of the Mafic Complex (Quick et al., 1994), these rocks are treated as having been rotated 90 degrees, so that their map pattern approximates a vertical cross section through the deep crust. The western intrusive contacts of the granitic bodies on either side of the Cremosina Line are also steeply dipping and for the purposes of this reconstruction are also treated as having been rotated 90 degrees from an initially subhorizontal orientation along with the Ivrea-Verbano Zone. The contact between the Valle Mosso granite and the overlying volcanic rocks dips approximately 35 degree to the east based on outcrop patterns and foliation in the granite near the contact. Based on our observations, and excluding local rotation of blocks near faults, attitudes on the volcanic are variable but dip in a generally eastward direction, ranging from about 30 in the west to 10 degrees in the easternmost exposures in the figure. Consistent with these dips, bedded limestone overlying volcanic rocks have shallow dips of 15 to 20 degrees. East of the Sesia Valley, the contact between volcanic rocks and schist dips approximately 60 degrees to the south.

(B) Removal of Quaternary and Tertiary cover and restoration of motion on north-northeast trending faults was performed south of the Cremosina Line. Fault motion was treated as predominantly normal and down to the west (Fantoni et al., 2003). The boundary of the caldera is inferred beneath the Po Plain.

(C) Restoration of motion on the Cremosina Line and Alpine faults north of the Cremosina Line. Based on the presence of sub-horizontal slickensides (Quick et al., 2003), restoration of the Cremosina faults was performed assuming purely strike-slip motion and matching contacts between the granites, Kinzigite Formation, and Mafic Complex. The restoration is consistent with the 12 km of dextral strike-slip offset reported by Boriani and Sacchi (1973), although we ignore 300 m of total normal motion that they infer for this system of faults as inconsequential at the scale at which we are working. Within our study area, Alpine faults north of the Cremosina Line have displacements less than 1 km based on displacement of mapped contacts (Quick et al., 2003).

(D) Removal of differential tilting. Volcanic and metamorphic rocks east of Roccapietra-Valle Mosso granite and easternmost granite were rotated into a vertical orientation with final thicknesses calculated on the basis of present day attitudes in the volcanic rocks, resulting in compression of their outcrop patterns. The top of the section corresponds to the dashed line in C. Normal faults cutting the floor of the caldera are schematic.

Figure A3: steps in the removal of Alpine and Mesozoic deformation in the southern Ivrea-Verbano Zone and Serie dei Laghi to reconstruct the early Permian crustal section. The pre-Permian CMB Line is projected from exposures north of the study area. Arrows indicate sense of displacement on faults with predominantly strike-slip motion; "U/D" indicates sense of displacement on faults with significant dip-slip motion. (A) Present-day geology. (B) Results of restoration of motion on normal faults south of the Cremosina Line. (C) Results of restoration of motion on the Cremosina Line and faults north of the Cremosina Line. (D) Results of removal of differential tilting.

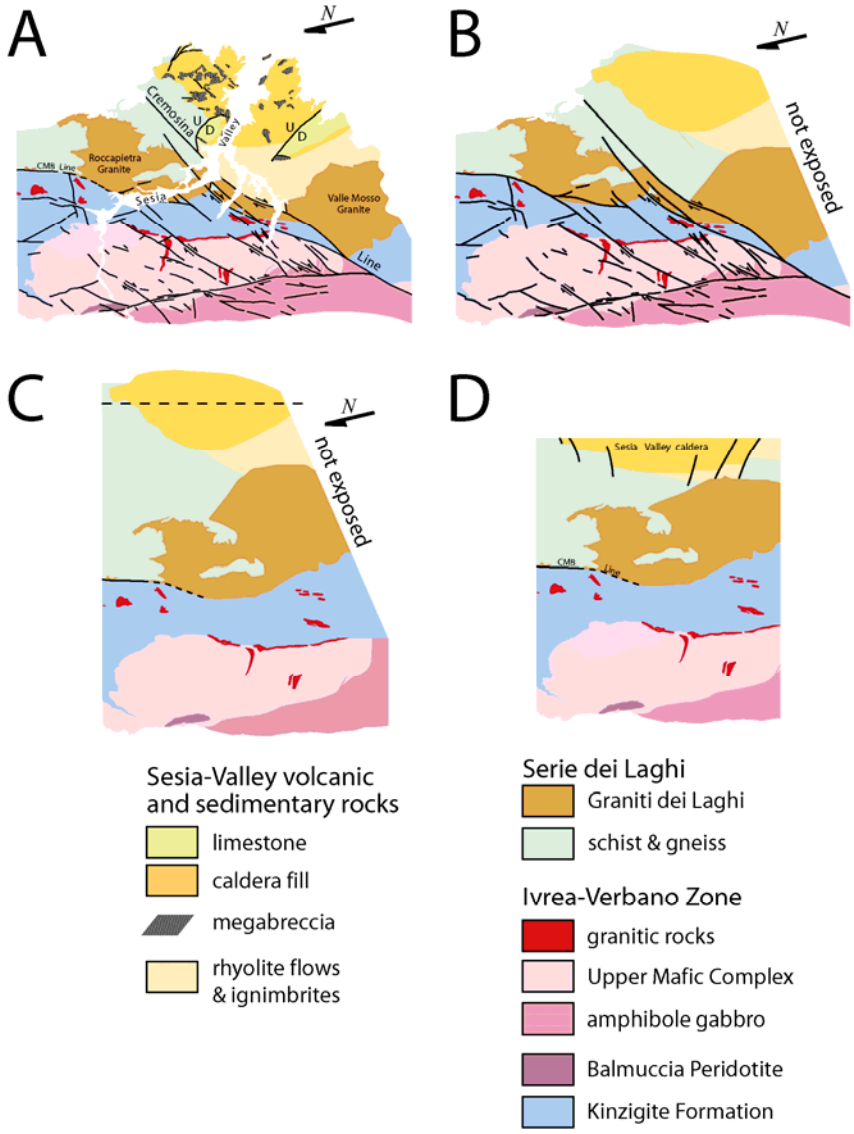

Construction of the Subsolidus synthetic seismic profiles

Subsolidus synthetic seismic profiles in Figure 4 were calculated using temperature- and pressure-dependent velocities measured on rocks of the Ivrea-Verbano Zone and Serie dei Laghi by Khazanehdari et al. (2000). In estimating the effects of the presence of partial melt, we note

that Hammond and Humphreys (1999) measured velocity reductions of 3.6 and 7.9 percent per percent melt for P and S waves, respectively, for peridotite. However, velocity reductions in crustal rocks are likely to be less due to smaller velocity contrasts with melts, and velocity reductions in Figure 4 due to the presence of residual melt in the Roccapietra granite and the Mafic Complex shortly after the caldera-forming event were estimated by assuming 7% residual interstitial melt and estimating velocity reductions of 1 and 2 percent per percent melt for P and S waves.

References Cited

Demarchi, G., Quick, J.E., Sinigoi, S., and Mayer, A., 1998, Pressure gradient and original orientation of a lower-crustal intrusion in the Ivrea-Verbano Zone, Northern Italy: Journal of Geology, v. 106, p. 609-622.

Boriani, A., and Sacchi, R., 1973, Geology of the junction between the Ivrea-Verbano and Strona-Ceneri Zones: Memorie dell'Istituto di Geologia e Mineralogia Università di Padova, v. 28, 36 pp..

Fantoni, R., Decarlis, A., and Fantoni, E. (2003). L'estensione mesozoica al margine occidentale delle Alpi Meridionali (Piemonte settentrionale, Italia): Atti Ticinensi di Scienze della Terra, v. 44, p. 97-110.

Hammond, W.C., and Humphreys, E.D., 1999, Upper mantle seismic wave velocity: Effects of realistic partial melt geometries: Journal of Geophysical Research, v. 105, p. 10,975-10,986.

Khazanehdari, J., rutter, E.H., and Brodie, K.H., 2000, High-pressure-high-temperature seismic velocity structure of the midcrustal and lower crustal rocks of the Ivrea-Verbano Zone and Serie dei Laghi, NW Italy: Journal of Geophysical Research, v. 105, p. 13,843-13858, doi: 10.1029/2000JB900025.

Peressini, G., Quick, J.E., Sinigoi, S., Hofmann, A.W., and Fanning, M., 2007, Duration of a Large Mafic Intrusion and Heat Transfer in the Lower Crust: a SHRIMP U/Pb Zircon Study in the Ivrea-Verbano Zone (Western Alps, Italy): Journal of Petrology, v. 48, p. 1185-1218.

Quick, J.E., Sinigoi, S., Snoke, A.W., Kalakay, T.J., Mayer, A., and Peressini, G., 2003, Geologic map of the southern Ivrea-Verbano Zone, northwestern Italy: U.S. Geological Survey, Reston, Virgina, VA, Geologic Investigations Series Map I-2776, scale 1:25 000, 1 sheet, 22 p. text.

Quick, J.E., S. Sinigoi, and A. Mayer, 1994, Emplacement dynamics of a large mafic intrusion in the lower crust, Ivrea-Verbano Zone, northern Italy: Journal of Geophysical Research, v. 99, p. 21,559-21,573.